An adaptive model predictive approach for automated vehicle control in fallback procedure based on virtual vehicle scheme

Wei Xue, Rencheng Zheng, Bo Yang, Zheng Wang and Tsutomu Kaizuka
Institute of Industrial Science, The University of Tokyo, Tokyo, Japan, and

Kimihiko Nakano
Institute of Industrial Science, The University of Tokyo, Tokyo, Japan and Interfaculty Initiative in Information Studies,
The University of Tokyo, Tokyo, Japan

Abstract

Purpose – Automated driving systems (ADSs) are being developed to avoid human error and improve driving safety. However, limited focus has been given to the fallback behavior of automated vehicles, which act as a fail-safe mechanism to deal with safety issues resulting from sensor failure. Therefore, this study aims to establish a fallback control approach aimed at driving an automated vehicle to a safe parking lane under perceptive sensor malfunction.

Design/methodology/approach – Owing to an undetected area resulting from a front sensor malfunction, the proposed ADS first creates virtual vehicles to replace existing vehicles in the undetected area. Afterward, the virtual vehicles are assumed to perform the most hazardous driving behavior toward the host vehicle; an adaptive model predictive control algorithm is then presented to optimize the control task during the fallback procedure, avoiding potential collisions with surrounding vehicles. This fallback approach was tested in typical cases related to car-following and lane changes.

Findings – It is confirmed that the host vehicle avoid collision with the surrounding vehicles during the fallback procedure, revealing that the proposed method is effective for the test scenarios.

Originality/value – This study presents a model for the path-planning problem regarding an automated vehicle under perceptive sensor failure, and it proposes an original path-planning approach based on virtual vehicle scheme to improve the safety of an automated vehicle during a fallback procedure. This proposal gives a different view on the fallback safety problem from the normal strategy, in which the mode is switched to manual if a driver is available or the vehicle is instantly stopped.

Keywords Model predictive control, Automated vehicles, Fallback, Sensor failure, Virtual vehicle scheme

Paper type Research paper

1. Introduction

The development of automated driving technologies is rapidly advancing. However, safety issues resulting from perceptive sensor failure are still crucial to automated driving safety (Harris, 2016). When perceptive sensor failure occurs during the automated driving procedure, it is necessary for human drivers or the automated driving system (ADS) to perform fallback behavior, which is to operate the automated vehicle as well as achieve a minimal risk condition (SAE On-Road Automated Vehicle Standards Committee, 2016). For the ADS at Levels 1-3, the human driver is assumed to perform the fallback maneuver, while at Level 4 or 5, the ADS can execute fallback behavior without human intervention. Therefore, this study focuses on the fallback procedure of an automated vehicle under front sensor failure without human intervention.

Currently available automated vehicles require a receptive human driver to a takeover request. Therefore, work has been conducted that explores the time and quality of driver intervention after the ADS issues a takeover request to reduce the risk during the shift from autopilot to manual driving mode (Braunagel *et al.*, 2017; Zeeb *et al.*, 2015). However, it is difficult to guarantee that the driver will always be available to take over the vehicle. Therefore, when an abrupt sensor failure event occurs, an advanced ADS not only has the ability to

instruct the driver to take over the vehicle but can also perform the fallback task without human assistance.

There has been research on safe fallback behavior performed by ADS. Emzivat et al. (2017) proposed a fallback strategy aimed at Level 4 ADS features designed to operate a vehicle on a road, whose ability to monitor the environment has been compromised. They considered a specific scenario where the visibility range of a driver is limited. Owing to the limited visibility range, a low-speed strategy was proved to be safer than an emergency stop. Svensson et al. (2018) proposed a trajectory planning method to safely stop a vehicle on a road shoulder, in which the safe stop problem was formulated as an optimal control problem. However, their method lacks consideration of moving obstacles; thus, it is not applicable to scenarios involving multiple vehicles. Little attention has been given to safe control of an automated vehicle for the fallback procedure in a dynamic driving environment.

Normally, a proper control algorithm for the fallback procedure is supposed to perform optimal vehicle control tasks under multiple constraints on road boundaries, traffic regulations, and collision avoidance. Research has shown that model predictive control (MPC) could be applied to build a theoretical framework of the constrained vehicle control problem (Mayne et al., 2000). MPC is designed to predict future responses based on a dynamic model of the control process, thereby anticipating future events and calculating optimal control actions. With the development of research on vehicle issues, MPC has exhibited great performance on vehicle control (Erlien et al., 2016; Falcone et al., 2007; Lima et al., 2017; Yang et al., 2018; Yoshida et al., 2008), trajectory planning (Howard, 2009; Li et al., 2014; Ji et al., 2017) and collision avoidance (Anderson et al., 2010; Liu et al., 2017).

In this study, a vehicle control problem was modeled with regard to the fallback event of an automated vehicle under sensor failure. Moreover, adaptive MPC is applied to the vehicle control in the fallback procedure. Normally, a vehicle control task requires explicit environmental information. Nevertheless, the environmental information is usually uncertain to the automated vehicle as a result of perceptive sensor failure in the fallback procedure. To maintain operation of the ADS, a prior prediction of the behavior of surrounding vehicles in the undetected area is necessary when perceptive sensor failure occurs. Therefore, this study applied a virtual vehicle scheme (Kim et al., 2009) to perform predictions of undetectable vehicles. The method has been applied in the longitudinal control of car-following (Kim, 2012; Liu et al., 2017) to smooth the vehicle motion control in lane-keeping scenarios. This study expands upon the implementation of the virtual vehicle scheme in dealing with abrupt sensor malfunction, using virtual vehicles to give a transitory prediction of the behavior of undetectable vehicles. The virtual vehicles fill the detection gap caused by sensor failure, thus, further enabling the ADS to predict the behavior of surrounding vehicles during the fallback process.

Furthermore, in this study, the vehicle control problem was modeled from highway traffic, including manually driven vehicles and an automated vehicle with abrupt perceptive sensor failure. Considering an undetectable area resulting from perceptive sensor failure, the virtual vehicle

scheme was developed to assist the ADS to complete the perception model of the driving environment. Based on the completed perception model, predictions of the subsequent variations in the surrounding driving environment as well as constraints on collision avoidance were made. Furthermore, a controller was developed from the adaptive MPC algorithm. The present paper is an improved version of our conference paper (Xue et al., 2018). We present an improved method including real-time consideration as well as a numerical analysis on additional fallback scenarios.

The rest of the paper is organized as follows. A fallback problem for an automated vehicle is described in Section 2. The vehicle model is presented in Section 3. Details of the proposed vehicle control approach are introduced in Section 4. The numerical analysis on the test scenarios is shown in Section 5. Finally, the conclusions drawn from the research are presented in Section 6.

2. Problem description

As illustrated in Figure 1, the host vehicle is assumed to lose its ability to collect environmental information ahead owing to front sensor malfunction while traveling in automated driving mode. As a result, an undetected area appears in front of the host vehicle. The host vehicle fails to read road signs or perceive obstacles in the undetected area. In response, the ADS immediately terminates the current driving task and executes the fallback maneuver. The detection delay of the sensor failure is neglected in this study because algorithms to reduce the fault detection delay have already been proposed, which can reduce the delay to a fairly low level for sensors with high sampling frequencies (Jeong et al., 2015; Kim, 1994). The complete fallback procedure comprises three phases under the problem setting: lane-keeping, lane change and pulling over. First, in the lane-keeping phase, the ADS adjusts the vehicle speed and keeps the host vehicle in the original lane while issuing a takeover request to the driver. Then, if no response is received, it may be necessary for the vehicle to change to the emergency parking lane and slow to a minimum cruise velocity. Finally, the host vehicle must be pulled over to the road shoulder. In this study, it is assumed that the driver is unable to respond to the takeover request. In addition, the pulling-over phase was not considered. Therefore, the problem focuses on the lane-keeping and lane-changing phases in the fallback procedure.

The problem is modeled on a straight road section of a two-lane, one-direction and left-hand expressway with a speed limit of

Figure 1 Illustration of the driving environment in a fallback event
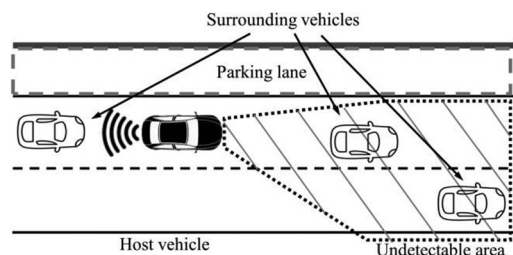
50-100 km/h. An emergency parking lane was the designated destination of the fallback procedure as soon as it was executed. The parking lane was marked in the embedded digital map of the host vehicle in advance, and it was assumed to be unoccupied during the fallback procedure. The surrounding vehicles are manually driven when sensor failure occurs and have no direct communication with the host vehicle. Normally, it is considered that potential collisions only occur between vehicles.

Despite front sensor failure, the side and rear perceptive sensors of the host vehicle are assumed to function well, guaranteeing the detection of road boundaries and rear vehicles. The ADS can collect the real-time positions and velocities of detected vehicles from the well-functioning sensors. Meanwhile, the localization module, for example, global positioning system, is assumed to be unaffected by the sensor failure during the fallback procedure. Moreover, the ADS is assumed to be equipped with high-precision digital map. Therefore, the host vehicle still retains the ability to perform lane-keeping and lane-changing behavior under sensor failure.

3. Vehicle model

This section presents a model of the host vehicle as a nonlinear dynamic system, while a linear and discrete model is derived from the nonlinear vehicle model for use of the MPC optimization process.

3.1 Vehicle modeling

As illustrated in Figure 2, the X-Y coordinates were fixed on the road and represent the longitudinal and transverse directions on the road, respectively. A 2-DOF bicycle model (Abe, 2015) was used to describe the vehicle dynamics, whose dynamic equations were established as follows:
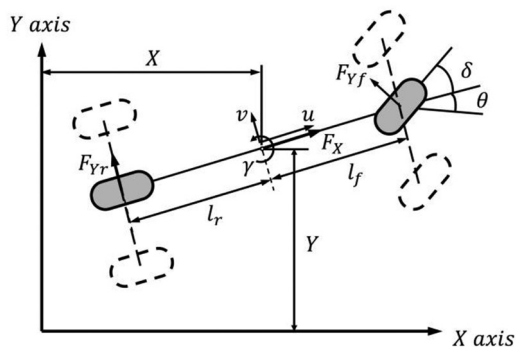
$$M(\dot{u} - v\gamma) = F_X \tag{1}$$

$$M(\dot{v} + u\gamma) = F_{Yf} + F_{Yr} \tag{2}$$

$$I_z \dot{\gamma} = l_f F_{Yf} - l_r F_{Yr} \tag{3}$$

$$\dot{\theta} = \gamma \tag{4}$$

$$\dot{X} = u\cos\theta - v\sin\theta \tag{5}$$

Figure 2 Illustration of vehicle model

$$\dot{Y} = v\cos\theta + u\sin\theta \tag{6}$$

where M is the total mass of the vehicle; u, v, and γ denote the longitudinal velocity, lateral velocity, and yaw rate of the vehicle at its center of gravity, respectively; F_X is the total longitudinal force on the tires; F_{Yf} and F_{Yr} represent the lateral forces on the front and rear tires, respectively; I_z is the yaw moment of inertia; l_f and l_r represent the distances from the vehicle's center of gravity to the front and rear axles, respectively; X and Y denote the longitudinal position and lateral position of the center of gravity of the vehicle; and θ is the heading angle with respect to the X-axis.

According to the tire model proposed by Fiala (1954), the lateral forces on tires are approximately described as follows:

$$F_{Yf} = C_f\left(\delta - \frac{v + l_f\gamma}{u}\right) \tag{7}$$

$$F_{Yr} = C_r\left(-\frac{v - l_r\gamma}{u}\right) \tag{8}$$

where C_f and C_r represent the cornering stiffness values of front and rear tires, respectively, and δ is the front steering angle.

The nonlinear vehicle model can be compactly defined from equations (1)- (8) as follows:

$$\dot{x} = F(x, u_c) \tag{9}$$

where $x = \begin{bmatrix} X & u & Y & v & \theta & \gamma \end{bmatrix}^T$ and $u_c = \begin{bmatrix} F_X & \delta \end{bmatrix}^T$

3.2 Model linearization and discretization

The nonlinear model, given in equation (9), can be linearized by a one-order Taylor series around the operating point $(x_s, u_{c,s})$ as follows:

$$\dot{x} \approx F(x_s, u_{c,s}) + \nabla F(x_s, u_{c,s})\begin{bmatrix} x - x_s \\ u_c - u_{c,s} \end{bmatrix} \tag{10}$$

where ∇ represents the gradient.

Rewriting equation (10) into state-space representation, we obtained the following continuous-time model:

$$\dot{x} = A(x_s)x + Bu_c + N(x_s) \tag{11}$$

where:

$$A(x_s) = \left[\frac{\partial F}{\partial x}\right]_{x_s}, B = \left[\frac{\partial F}{\partial u_c}\right]_{u_{c,s}} = \begin{bmatrix} 0 & \frac{1}{M} & 0 & 0 & 0 & 0 \\ 0 & 0 & 0 & \frac{C_f}{M} & 0 & \frac{l_f C_f}{I_z} \end{bmatrix}^T$$

$$N(x_s) = F(x_s, u_{c,s}) - A(x_s)x_s - Bu_{c,s}.$$

By discretizing the continuous-time model over a sample time T_s, equation (11) was transformed into a discrete state-space representation as follows:

$$x_{k+1} = A_d(x_s)x_k + B_d(x_s)u_{c,k} + N_d(x_s) \tag{12}$$

where $A_d(x_s) = e^{A(x_s)T_s}$, $B_d(x_s) = \int_0^{T_s} e^{A(x_s)\tau}Bd\tau$ and $N_d(x_s) = \int_0^{T_s} e^{A(x_s)\tau}N(x_s)d\tau$.

4. Control algorithm

This section presents the development of the adaptive model predictive controller for the fallback procedure. The virtual vehicle scheme was implemented to complete the perception model of the surrounding driving environment, introduced in Section 4.1. Predictions of the behavior of surrounding vehicles were developed for the construction of safe driving constraints, as in Section 4.2. The desired control outputs are defined in Section 4.3, including the desired longitudinal velocity and lateral trajectory in the fallback procedure. Finally, a model predictive controller was formulated as in Section 4.4.

4.1 Virtual vehicle scheme

Front vehicles become undetectable to the host vehicle owing to front sensor malfunction. Therefore, the virtual vehicle scheme was implemented to give a prediction of the movement of the undetected front vehicles. As illustrated in Figure 3, when the ADS fails to detect front vehicles owing to sensor failure, the same number of virtual vehicles is created to replace each undetected vehicle. The virtual vehicle inherits the position and velocity from the history data of its corresponding undetected vehicle.

To reduce the collision risk during the fallback procedure, the control algorithm should anticipate the most dangerous driving behavior that the undetected vehicles would take and further manage to avoid accidents under these conditions. Therefore, virtual vehicles are assumed to approach the host vehicle in hazardous ways. The prediction of the velocity of a virtual vehicle is illustrated in Figure 4. The virtual vehicle is assumed to decelerate at a maximum deceleration until a stop if it is in the same lane as the host vehicle, which is the most dangerous manner to approach the host vehicle. The velocity profile of a virtual vehicle, v_f, is defined as follows:

$$v_f(t) = \max(v_f(t_0) - a_m(t - t_0), 0),\ t > t_0 \tag{13}$$

where t_0 denotes the time when sensor failure occurs and a_m is the maximum deceleration of the virtual vehicle.
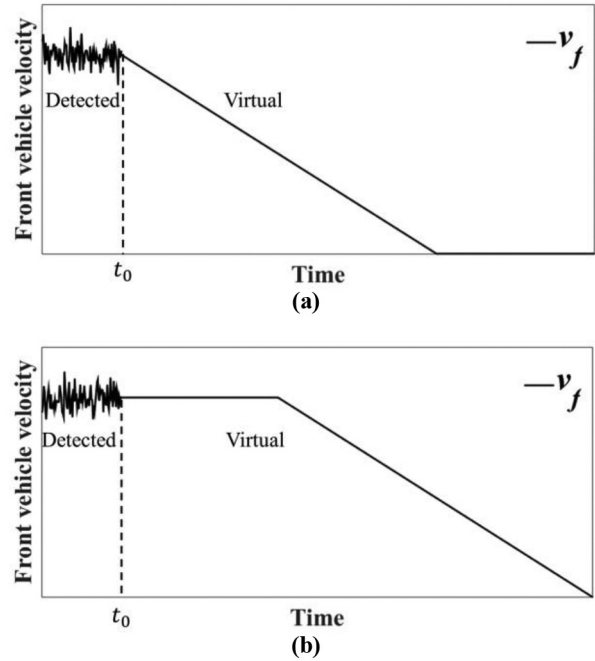
If the virtual vehicle is in another lane, it is assumed to maintain its initial speed and change to the lane of the host

Figure 3 Explanations of virtual vehicle schemes
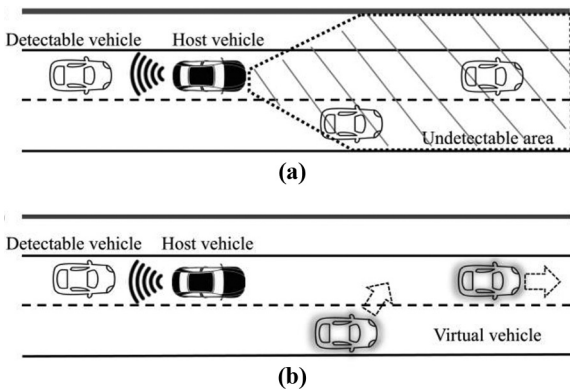
Notes: (a) Sensor failure resulting in undetected area; (b) virtual vehicles replacing undetected vehicles

Figure 4 Velocity prediction of the virtual vehicle

Notes: (a) Velocity prediction when the front vehicle is in the same lane as the host vehicle; (b) velocity prediction when the front vehicle is in a different lane to the host vehicle

vehicle before decelerating at maximum deceleration until it reaches a stop. The velocity profile is defined as follows:

$$v_f(t) = \begin{cases} v_f(t_0), & t_0 < t \leq t_d \\ \max\big(v_f(t_0) - a_m(t - t_d),\, 0\big), & t > t_d \end{cases} \tag{14}$$

where t_d is the time delay assumed for the lane change. The delay is considered for two reasons. First, a driver rarely decelerates significantly while changing lane; second, vehicles in different lanes may not have enough longitudinal space, the delay gives the host vehicle time to make space for the sudden cutting-in behavior of the virtual vehicle.

Although a short-term traffic prediction method, for example, long short-term memory network (Zhao *et al.*, 2017) may match the driving behavior of the front vehicle in most of the cases that method can hardly predict an abrupt dangerous behavior of the front vehicle. In this work, the most dangerous condition is taken into consideration, to make the host vehicle avoid all the potential collisions with undetectable vehicles.

4.2 Safe driving constraints

The safe driving constraints were built upon the predictions of the surrounding vehicles. The constraints were considered up to a maximum prediction step, n_p. Here, n_p is named the prediction horizon.

The prediction of the velocity of the front vehicle up to the prediction horizon was determined based on the velocity profile in equation (13) as follows:

$$\hat{v}_{f,k+i} = v_f(t_{k+i}), \ i = 1, \ldots, n_p \tag{15}$$

where k denotes the current timestep and i is the prediction step. The notation "^" represents that the marked variable is a prediction.

The rear vehicle was assumed to keep following the host vehicle, while responding to the velocity variation of the host vehicle after a short delay. Therefore, the prediction of the rear vehicle follows the car-following model proposed by Chandler *et al.* (1958), as shown below:

$$\hat{\dot{v}}_{r,k+i} = \lambda \left(u_{k+i-n_p} - v_{r,k+i-n_p} \right), i = 1, \ldots, n_p \tag{16}$$

where v_r represents the velocity of the rear vehicle; $\hat{\dot{v}}_r$ is the prediction of the acceleration of the rear vehicle; and λ is a constant parameter.

The safe driving constraints were defined based on the time-to-collision (TTC) values between the host vehicle and surrounding vehicles as follows:

$$\mathrm{TTC}_{\alpha,k+i} \geq T_{safe} - i \cdot T_s, \ \ \alpha \in \{f, r\},$$
$$i = 1, \ldots, n_p, \tag{17}$$

$$\mathrm{TTC}_{f,k+i} = \frac{\hat{X}_{f,k+i} - \hat{X}_{k+i} - L_f}{\hat{u}_{k+i} - \hat{v}_{f,k+i}} \tag{18}$$

$$\mathrm{TTC}_{r,k+i} = \frac{\hat{X}_{k+i} - \hat{X}_{r,k+i} - L_r}{\hat{v}_{r,k+i} - \hat{u}_{k+i}} \tag{19}$$

where TTC_α, for $\alpha \in \{f, r\}$, denotes the TTC value between the host vehicle and the front vehicle or rear vehicle; X_f and X_r are the longitudinal positions of the front vehicle's back and the rear vehicle's front, respectively; $\hat{X}_f$ and $\hat{X}_r$ were derived from the predictions of the velocities of the front and rear vehicles, respectively; L_f and L_r denote the distances from the center of gravity of the host vehicle to its front and back, respectively; and T_{safe} represents the safe TTC value.

The safe driving constraints take effect until the host vehicle completely leaves the active lane. Consequently, the safe driving constraints can be defined in a discrete representation during the prediction horizon interval as follows:

$$E_i \hat{x}_{k+i} \leq h + D_i \hat{w}_{k+i}, \quad i = 1, \ldots, n_p \tag{20}$$

where
$$h = \begin{bmatrix} -L_f & -L_r \end{bmatrix}^T, \hat{w} = \begin{bmatrix} \hat{X}_f & \hat{v}_f & \hat{X}_r & \hat{v}_r \end{bmatrix}^T;$$
$$E_i = \begin{bmatrix} 1 & T_{safe} - i \cdot T_s & 0 & 0 & 0 & 0 \\ -1 & -T_{safe} + i \cdot T_s & 0 & 0 & 0 & 0 \end{bmatrix}; \text{ and}$$
$$D_i = \begin{bmatrix} 1 & T_{safe} - i \cdot T_s & 0 & 0 \\ 0 & 0 & -1 & -T_{safe} + i \cdot T_s \end{bmatrix}.$$

4.3 Determination of desired outputs

It is assumed that the desired velocity and lane were predefined in an optimization problem for tracking. Therefore, the longitudinal velocity and lateral position of the host vehicle's center of gravity are the outputs to be tracked:

$$y = \begin{bmatrix} u & Y \end{bmatrix}^T = Cx,$$
$$C = \begin{bmatrix} 0 & 1 & 0 & 0 & 0 & 0 \\ 0 & 0 & 1 & 0 & 0 & 0 \end{bmatrix} \tag{21}$$

$$y_{des} = \begin{bmatrix} u_{des} & Y_{des} \end{bmatrix}^T, \tag{22}$$

where y is the vector of the output variables; y_{des} is the vector of the desired outputs; and u_{des} and Y_{des} are the desired longitudinal velocity and lateral position, respectively.

The lane-keeping and lane-changing phases were considered. During the lane-keeping phase, the host vehicle decelerates along the active lane, waiting for a possible takeover from the driver. After this, the vehicle enters the lane-changing phase, changing to the emergency parking lane and slowing, ready to be pulled over to the road shoulder.

The time to switch from the lane-keeping phase to the lane-changing phase is denoted as t_l. When $t_0 < t < t_l$, the desired outputs are defined as follows:

$$u_{des}(t) = \max(u(t_0) + a_{des}(t - t_0), v_{c,min}),$$
$$Y_{des}(t) = Y(t_0) \tag{23}$$

where $u(t_0)$ and $Y(t_0)$ are the longitudinal velocity and the lateral position of the host vehicle when sensor failure occurs, respectively; $v_{c,min}$ is the minimum cruising speed; and a_{des} is the desired acceleration.

When $t \geq t_l$, the desired outputs in the lane-changing phase are defined as follows:

$$u_{des}(t) = \max(u(t_0) + a_{ref}(t - t_0), v_{c,min}),$$
$$Y_{des}(t) = \begin{cases} P(t), & t_l \leq t < t_l + T_{lc} \\ L_w + Y(t_0), & t \geq t_l + T_{lc} \end{cases},$$
$$P(t) = L_w \left[6 \left(\frac{t - t_l}{T_{lc}} \right)^5 - 15 \left(\frac{t - t_l}{T_{lc}} \right)^4 + 10 \left(\frac{t - t_l}{T_{lc}} \right)^3 \right] + Y(t_0) \tag{24}$$

where Y_{des} was designed based on a quintic polynomial on time $P(t)$; L_w represents the lane width; and T_{lc} is the desired time cost of the lane change. The quintic polynomial is implemented to generate a smooth lateral position target, satisfying the position, lateral velocity and lateral acceleration constraints at both ends of the lateral position trajectory.

4.4 Adaptive model predictive control

The model predictive controller predicts the response of the vehicle up to a prediction horizon, and it optimizes a predefined objective function with constrained control inputs and outputs up to that horizon based on the predicted values. For a nonlinear system, the adaptive MPC (Giselsson, 2010) and nonlinear MPC (Borrelli *et al.*, 2005; Du *et al.*, 2016) are two major methods that resolve the nonlinear optimization problem. The adaptive MPC updates the embedded model with an approximate linear model in each optimization iteration, which has a lower computation cost than nonlinear MPC.

A diagram of the adaptive MPC is illustrated in Figure 5. Based on the measured state, an approximate linear model was generated to update the embedded model in the

Figure 5 Diagram of adaptive MPC scheme
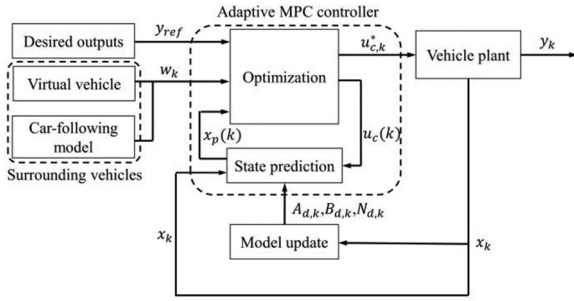
controller. By means of the embedded model, the MPC predicts future behaviors of the host vehicle. This prediction determines the future states within a specified prediction horizon, and based on these future states, control inputs are optimized to force the constrained output variables to track the predefined references.

The model update in each optimization iteration is based on the state variables of the vehicle as follows:

$$x_{k+1} = A_{d,k}x_k + B_{d,k}u_{c,k} + N_{d,k} \qquad (25)$$

where $A_{d,k} = A_d(x_k)$, $B_{d,k} = B_d(x_k)$, and $N_{d,k} = N_d(x_k)$.

Using the model in equation (25), the MPC was designed to predict the future state variables during the prediction horizon interval, $[1, n_p]$, through the current state variables and the control inputs. Note that the control inputs only change during the control horizon interval and remain constant after that, that is, $u_{c,k+i} = u_{c,k+n_c-1}$ for $n_c \leq i \leq n_p - 1$, in which n_c denotes the control horizon. The vectors of the predictive state variables $x_p(k)$ and control inputs $u_c(k)$ are represented by:

$$x_p(k) = \begin{bmatrix} \hat{x}_{k+1} & \hat{x}_{k+2} & \cdots & \hat{x}_{k+n_p} \end{bmatrix}^T \qquad (26)$$

$$u_c(k) = \begin{bmatrix} u_{c,k} & u_{c,k+1} & \cdots & u_{c,k+n_c-1} \end{bmatrix}^T \qquad (27)$$

The predictive state variables during the prediction horizon interval can be formulated as follows:

$$x_p(k) = \Psi_k x_k + \Theta_k u_c(k) + \Lambda_k N_{d,k} \qquad (28)$$

where $\Psi_k = \begin{bmatrix} A_{d,k} & A_{d,k}^2 & \cdots & A_{d,k}^{n_p} \end{bmatrix}^T$,

$$\Theta_k = \begin{bmatrix} B_{d,k} & 0 & \cdots & 0 \\ A_{d,k}B_{d,k} & B_{d,k} & \cdots & 0 \\ \vdots & \vdots & \ddots & \vdots \\ A_{d,k}^{n_c-1}B_{d,k} & A_{d,k}^{n_c-2}B_{d,k} & \cdots & B_{d,k} \\ \vdots & \vdots & \ddots & \vdots \\ A_{d,k}^{n_p-1}B_{d,k} & A_{d,k}^{n_p-2}B_{d,k} & \cdots & A_{d,k}^{n_p-n_c}B_{d,k} \end{bmatrix}, \text{ and}$$

$$\Lambda_k = \begin{bmatrix} I \\ A_{d,k} \\ \vdots \\ A_{d,k}^{n_p-1} \end{bmatrix}$$

Discretizing the desired outputs predefined in equations (22)-(24), the vehicle control problem can be transformed into the following optimization problem:

$$\min \sum_{i=1}^{n_p} (\hat{y}_{k+i} - y_{des,k+i})^T Q(\hat{y}_{k+i} - y_{ref,k+i})$$

$$+ \sum_{i=0}^{n_c-1} u_{c,k+i}^T R u_{c,k+i} + \sum_{i=0}^{n_c-1} \Delta u_{c,k+i}^T S \Delta u_{c,k+i} + \rho_\varepsilon \varepsilon^2$$

$$(29a)$$

$$s.t. \ E_{i+1}\hat{x}_{k+i+1} \leq h + D_{i+1}\hat{w}_{k+i+1} + \varepsilon V \qquad (29b)$$

$$y_{min} \leq \hat{y}_{k+i+1} \leq y_{max} \qquad (29c)$$

$$u_{c,min} \leq u_{c,k+i} \leq u_{c,max} \qquad (29d)$$

$$\Delta u_{c,min} \leq \Delta u_{c,k+i} \leq \Delta u_{c,max} \qquad (29e)$$

$$\varepsilon \geq 0 \qquad (29f)$$

$$i = 0, 1, \ldots, n_p - 1 \qquad (29g)$$

where $\hat{y}_{k+i} = C\hat{x}_{k+i}$, which is the vector of the predictive output variables; Q, R and S represent the weight matrices on the outputs, inputs, and input increments, respectively; and $\Delta u_{c,k+i}$ represents the discrete input increment. The constraint of equation (29b) is a soft constraint extended from equation (20), implying that the constraint violation is allowed but that violation is penalized in the objective function. ε is a slack variable to allow the constraint violation, and ρ_ε is the weight on the penalty for constraint violation. The vector V is the band for constraint softening, which is used to adjust the strictness of each constraint. A larger band represents less penalty on the constraint violation, while a zero band does not allow any constraint violation. The constraint of equation (29c) was determined owing to the traffic regulations on speed limits and road boundaries in specific scenarios.

The MPC optimization problem in equation (29) can be transformed into a quadratic programming problem. The sequence of the optimal input can be obtained through a quadratic programming solver as follows:

$$u_c^*(k) = \begin{bmatrix} u_{c,k}^* & u_{c,k+1}^* & \cdots & u_{c,k+n_c-1}^* \end{bmatrix}^T \qquad (30)$$

where $u_{c,k}^*$ is transferred to the vehicle plant as the optimal control input at the current timestep.

5. Case studies

5.1 Test scenarios

In this study, four test scenarios were defined to test the performance of the proposed approach. The test scenarios represent only some of the many cases that could occur when the automated vehicle encounters front sensor failure. Nevertheless, these scenarios can evaluate the performance of the proposed approach in avoiding rear-end collisions with surrounding vehicles during the lane-keeping and lane-changing phases in the fallback procedure.

In each scenario, the surrounding vehicles were modeled as double integrators whose input is acceleration and outputs are

position and velocity. A virtual vehicle was created upon the initial position and velocity of the front vehicle, and it was set to behave in a hazardous way, as described in Section 4.1. The rear vehicle in each scenario was set to maintain its original speed within the first 2.4 s, and decelerate to 50 km/h at a constant deceleration a_r. This driver reaction time was chosen according to the study result that over 95 per cent of drivers take less than 2.4 s to react with an unalert deceleration of the front vehicle (Taoka, 1989). The ADS adopted a fixed fallback strategy that the host vehicle keeps in the initial lane within the first 3 s waiting for the driver to take over and then moves to the emergency parking lane for a low-speed cruise.

Scenarios 1 and 2 were developed from a car-following case, as illustrated in Figure 6(a). In Scenario 1, there is a short car-following distance between the host vehicle and the rear vehicle. The host vehicle should follow the desired longitudinal velocity to decelerate during the lane-keeping phase, while the rear vehicle does not react sufficiently to the sudden deceleration of the host vehicle and decelerates slower than expected. Therefore, the host vehicle may need to decrease the brake pedal force to avoid a collision with the rear vehicle. In Scenario 2, there is a short car-following distance between the host vehicle and the front vehicle. A virtual vehicle was created on the initial position of the front vehicle, and it was supposed to decelerate at the maximum deceleration. The host vehicle may need to follow a velocity profile lower than the desired velocity profile before leaving the active lane.

Scenarios 3 and 4 test the performances of the proposed method in an overtaken and overtake case, respectively, as illustrated in Figure 6(b). In Scenario 3, the host vehicle is overtaken by the front vehicle in the right lane. In Scenario 4, the host vehicle overtakes the front vehicle in the right lane at a velocity 20 km/h higher than that of the front vehicle, just before executing a fallback behavior. The host vehicle may need to avoid a potential collision brought by the sudden cut-in behavior of the front vehicle. In both scenarios, the host vehicle may need to keep a safe distance with the rear vehicle, as well.

Figure 6 Illustration of test scenarios
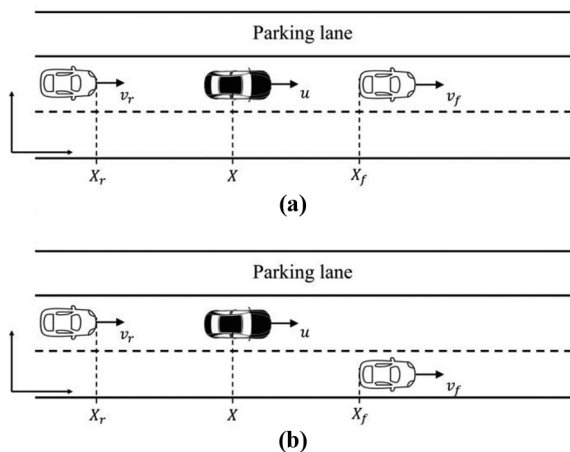
Notes: (a) Car-following cases in scenarios 1 and 2;
(b) overtaking and overtaken cases in scenarios 3 and 4

The initial parameters of the test scenarios are listed in Table I, including the initial positions and velocities of the rear, host and front vehicles as well as the deceleration of the host vehicle.

The numerical results are obtained by a simulation procedure conducted in a Simulink and CarSim environment. The MPC controller is programmed with Simulink tools, and the plant of host vehicle is a Mercedes-Benz B-class hatchback model, whose parameters were extracted from CarSim database. The controller parameters are listed in Table II.

5.2 Numerical analysis

The analysis results of Scenario 1 are illustrated in Figure 7. The path of the host vehicle is illustrated in Figure 7(a). In this figure, the colored markers describe the positions of the host vehicle, rear vehicle and virtual front vehicle at four sample times. Different vehicles are represented by different shapes, and each color represents a sample time. As it is shown, the host vehicle maintains its position in the original lane within the first 3 s and then changes to the parking lane after. The host vehicle maintains a short distance with the rear vehicle until it leaves the lane at 5.8 s. As illustrated in Figure 7(d), the host vehicle decelerates along the desired velocity at the beginning of the fallback procedure but later maintains its speed for a short while to avoid a close separation with the rear vehicle, until leaving the active lane. As illustrated in Figure 7(e), before the host vehicle leaves the active lane, the minimum TTC value with the rear vehicle is 2.74 s. Because the safe driving constraint is a soft constraint, the constraint violation will not result in an infeasible solution to the

Table I Test scenario parameters

	X_f (m)	X_r (m)	u (km/h)	v_f (km/h)	v_r (km/h)	a_r (m/s^2)
Scenario 1	90	−45	90	90	90	2.0
Scenario 2	50	−60	90	90	90	2.5
Scenario 3	20	−60	90	70	90	2.5
Scenario 4	5	−70	90	95	90	2.5

Table II Parameters of the path-planning controller

Symbol	Value (unit)	Symbol	Value (unit)
M	1230 (kg)	I_z	1343.1 (kgm^2)
C_f	100800 (N)	C_r	70800 (N)
l_f	1.04 (m)	l_r	1.56 (m)
L_f	1.70 (m)	L_r	2.26 (m)
a_m	5 (m/s^2)	t_d	3 (s)
λ	0.4 (s^{-1})	$a_{\backslash bie \backslash}$	−2.5 (m/s^2)
L_w	3.5 (m)	t_l	3 (s)
T_{lc}	4 (s)	$v_{c,min}$	18 (km/h)
T_{safe}	4 (s)	t_0	0 (s)
T_s	0.05 (s)	$\rho_{\backslash ill \backslash}$	10^5
n_p	40	n_c	5
Q	diag (6, 100)	R	diag (7e−7,10)
S	diag (4e−7,8e5)	V	[10,10,0]^T
y_{min}	[0, −5]^T	y_{max}	[27.8, 4.25]^T
$u_{c,min}$	[−6150, −0.2]^T	$u_{c,max}$	[6150, 0.2]^T
$\Delta u_{c,min}$	[−308, −0.02]^T	$\Delta u_{c,max}$	[308, 0.02]^T

Figure 7 Numerical analysis results of scenario 1
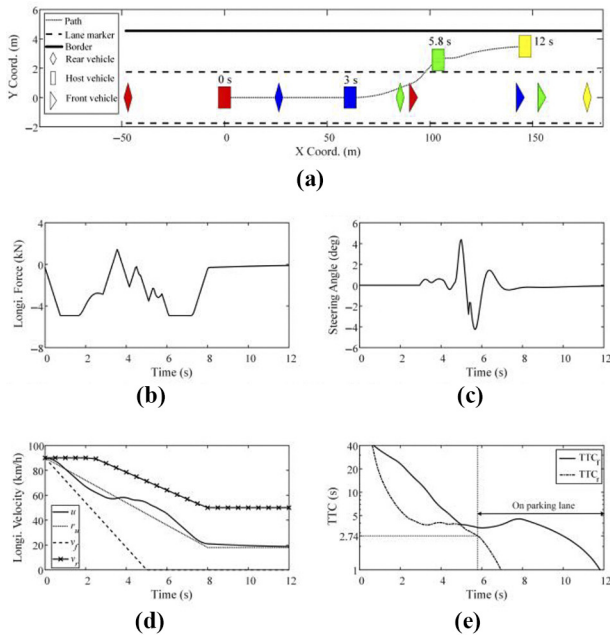
(a)

(b)   **(c)**

(d)   **(e)**

Notes: (a) Positions of the host vehicle (rectangle), the rear vehicle (diamond), and the virtual front vehicle (triangle) at different sample times: 0 s (red), 3 s (blue), 5.8 s (green), and 12 s (yellow); (b) longitudinal force input of the host vehicle; (c) front steer angle of the host vehicle; (d) longitudinal velocity profile; (e) TTC values between the host vehicle and surrounding vehicles

Figure 8 Numerical analysis results of scenario 2
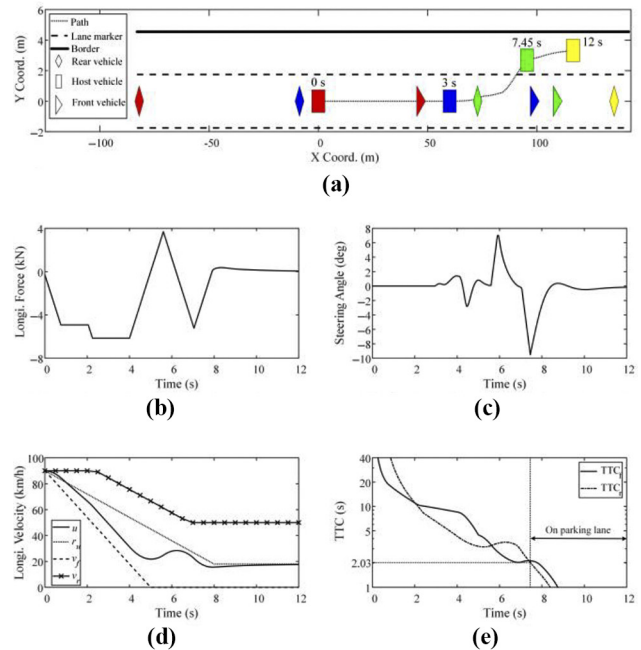

(a)

(b)   **(c)**

(d)   **(e)**

Notes: (a) Positions of the host vehicle (rectangle), the rear vehicle (diamond), and the virtual front vehicle (triangle) at four sample times: 0 s (red), 3 s (blue), 7.45 s (green), and 12 s (yellow); (b) longitudinal force input of the host vehicle; (c) front steer angle of the host vehicle; (d) longitudinal velocity profile; (e) TTC values between the host vehicle and surrounding vehicles

quadratic programming problem. Therefore, the controller still works even if the safe driving constraint is violated.

Scenario 2 describes a dense car-following case, whose numerical analysis results are illustrated in Figure 8. As can be seen in Figure 8(a), the host vehicle starts the lane-changing phase at 3 s and leaves the left lane completely at 7.45 s. Figure 8(d) illustrates the velocity profiles of the three vehicles in this scenario. The host vehicle makes a sharp deceleration to avoid a potential collision with the virtual front vehicle. Before the host vehicle leaves the active lane, the TTC values with the front and rear vehicle remain above 2.03 s, as illustrated in Figure 8(e).

Scenario 3 is an overtaken case, whose numerical analysis results are illustrated in Figure 10. The host vehicle completely leaves the middle lane until 7.55 s. From the velocity graph illustrated in Figure 10(d) and the TTC values illustrated in Figure 10(e), it is implied that the fast front vehicle has little influence on the control of the host vehicle. When the host vehicle travels into the middle lane, the TTC value with the front vehicle is higher than the safe TTC value in the safe driving constraint, while the minimum TTC value with the rear vehicle is slightly lower than the safe TTC value.

Scenario 4 was developed from an overtaking case. The positions of the host vehicle and surrounding vehicles are illustrated in Figure 9(a). In this figure, the virtual front vehicle cuts into the left lane within the first 3 s, before braking to a stop after. As illustrated in Figure 9(d), the front vehicle maintains a

lower velocity than its following vehicle in the first 3 s and then decelerates to a full stop. Owing to the dangerous cut-in behavior, the host vehicle sharply decelerates, as illustrated in Figure 9(d). The velocity of the host vehicle is mostly lower than the desired velocity before the host vehicle leaves the active lane, indicating that the host vehicle takes a hard brake to avoid the potential collision with the virtual vehicle. The host vehicle leaves the lane at 7.9 s, and the TTC value between the host vehicle and the front vehicle remains above 1.41 s.

In general, encounters of vehicles with a minimum TTC, of less than 1.5 s, are considered critical (Horst and Hogema, 1993). The numerical analysis shows that in the four test scenarios, the proposed method avoid collisions with the surrounding vehicles during fallback procedures. In Scenarios 1, 2 and 3, the host vehicle maintains relative safe separations to the surrounding vehicles, with minimum TTCs larger than the critical value. The TTC in Scenario 4 indicates that the host vehicle encounters a critical situation before leaving the active lane, as a result of the 3-second waiting time for driver response, which is too long in that situation. It is necessary to adjust the fallback strategy according to different fallback situations, and furthermore, the proposed approach can be applied to evaluate fallback strategies during the fallback procedure.

The average calculation time of an optimization iteration was 0.0131 s over all the test scenarios and therefore the control problem can be solved in real time, because the sample time is 0.05 s.

Figure 9 Numerical analysis results of scenario 3
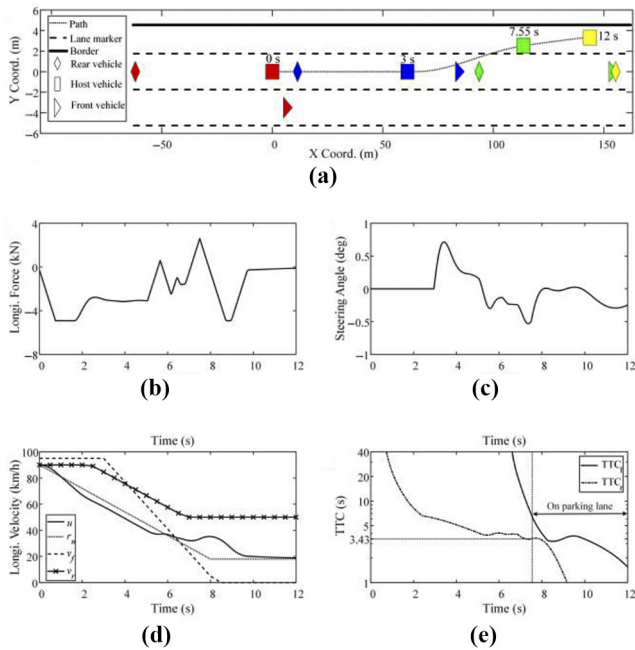
(a)

(b)

(c)

(d)

(e)

Notes: (a) Positions of the host vehicle (rectangle), the rear vehicle (diamond), and the virtual front vehicle (triangle) at four sample times: 0 s (red), 3 s (blue), 7.55 s (green), and 12 s (yellow); (b) longitudinal force input of the host vehicle; (c) front steer angle of the host vehicle; (d) longitudinal velocity profile; (e) TTC values between the host vehicle and surrounding vehicles

Figure 10 Numerical analysis results of scenario 4

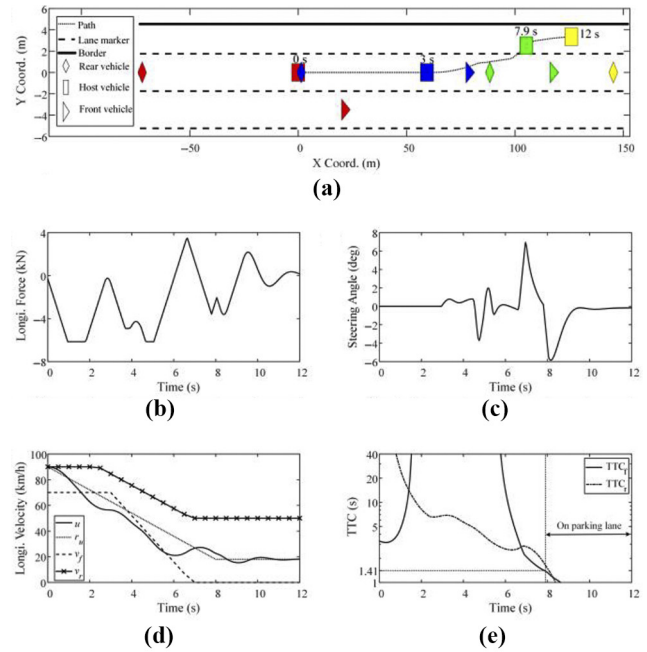**(a)**

(b)

(c)

(d)

(e)

Notes: (a) Positions of the host vehicle (rectangle), the rear vehicle (diamond), and the virtual front vehicle (triangle) at four sample times: 0 s (red), 3 s (blue), 7.9 s (green), and 12 s (yellow); (b) longitudinal force input of the host vehicle; (c) front steer angle of the host vehicle; (d) longitudinal velocity profile; (e) TTC values between the host vehicle and surrounding vehicles

6. Conclusions

This paper proposes an adaptive model predictive approach based on virtual vehicle scheme, to realize a fallback procedure of an automated vehicle while encountering a front perceptive sensor failure during highway transportation. To design the fallback procedure, the automated vehicle is normally required to perform lane-keeping and lane-changing behaviors, until safely reaching a low cruise speed in the emergency parking lane. Therefore, it was assumed that the undetectable vehicles continually perform hazardous driving behaviors, which may oblige the host vehicle to actively avoid incoming collisions.

In the beginning, virtual vehicles can be established from the history data to replace the surrounding vehicles in undetectable areas, then, an adaptive MPC controller is implemented to optimize the velocity and steering control for the fallback procedure. Furthermore, to reduce the computation cost brought by the nonlinear vehicle model, the embedded model in MPC is updated by a linearized discrete vehicle model at each optimization iteration. In this manner, the MPC optimization process can be solved as a real-time quadratic programming problem.

As a common sense, it is considered to be a safe fallback strategy that a human driver takes over the vehicle. However, driving automation causes drowsiness, which may lead to a late take-over response from the driver (Thiffault and Bergeron,

2003). Moreover, several traffic accident reports already showed that human drivers can easily make mistakes after taking over the vehicle under critical conditions (Favarò *et al.*, 2017). Therefore, it is still necessary for ADS to require a performing capability of fallback behavior. Anyway, to ensure driving safety of automated vehicles, different fallback strategies should be preserved in ADS for a variety of traffic conditions.

On the other hand, a hard brake to stop is commonly used as the fallback strategy in low-speed scenarios or when the ego vehicle encounters inevitable collision (Jain *et al.*, 2019). In high-speed traffic environment, an abrupt stop in an active lane probably results in rear-end collisions. Therefore, Emzivat *et al.* (2017) verified that a low-speed cruise strategy is safer than an emergency stop, when the speed limit is up to 70 km/h. For the highway case that emergency parking areas are normally set up, an alternative solution may be necessary to drive the automated vehicles to the emergency parking area.

Thereby, the proposed method takes an emergency parking area as the objective, while focuses on the steering and velocity control during the fallback process. This study further indicates that the proposed approach is effective for the driving safety of automated vehicles, even only regarding the front perceptive sensors. Compared with the emergency stop strategy and the low-speed cruise strategy, the strategy proposed in this study can reduce the subsequent impact on highway traffic. Additionally, it may be an interesting topic to evaluate the

vehicle control approach for a more complicated failure situation in a mixed transport environment.

References

Abe, M. (2015), *Vehicle Handling Dynamics: Theory and Application*, Butterworth-Heinemann, Oxford.

Anderson, S., Peters, S., Pilutti, T. and Lagnemma, K. (2010), "An optimal-control-based framework for trajectory planning, threat assessment, and semi-autonomous control of passenger vehicles in hazard avoidance scenarios", *International Journal of Vehicle Autonomous Systems*, Vol. 8 Nos 2/3/4, pp. 190-216.

Borrelli, F., Falcone, P. and Keviczky, T. (2005), "MPC-based approach to active steering for autonomous vehicle systems", *International Journal of Vehicle Autonomous Systems*, Vol. 3 Nos 2/3/4, pp. 265-291.

Braunagel, C., Rosenstiel, W. and Kasneci, E. (2017), "Ready for take-over? A new driver assistance system for an automated classification of driver take-over readiness", *IEEE Intelligent Transportation Systems Magazine*, Vol. 9 No. 4, pp. 10-22.

Chandler, R., Herman, R. and Montroll, E. (1958), "Traffic dynamics: studies in car-following", *Operations Research*, Vol. 6 No. 2, pp. 165-184.

Du, X., Htet, K. and Tan, K. (2016), "Development of a genetic-algorithm-based nonlinear model predictive control scheme on velocity and steering of autonomous vehicles", *IEEE Transactions on Industrial Electronics*, Vol. 63 No. 11, pp. 6970-6977.

Emzivat, Y., Ibanez-Guzman, J., Martinet, P. and Roux, O. (2017), "Dynamic driving task fallback for an automated driving system whose ability to monitor the driving environment has been compromised", in *Proceedings of IEEE Intelligent Vehicles Symposium*, Los Angeles, CA, pp. 1841-1847.

Erlien, S., Fujita, S. and Gerdes, J. (2016), "Shared steering control using safe envelopes for obstacle avoidance and vehicle stability", *IEEE Transactions on Intelligent Transportation Systems*, Vol. 17 No. 2, pp. 441-451.

Falcone, P., Borrelli, F., Asgari, J., Tseng, H. and Hrovat, D. (2007), "Predictive active steering control for autonomous vehicle systems", *IEEE Transactions on Control Systems Technology*, Vol. 15 No. 3, pp. 566-580.

Favarò, F., Nader, N., Eurich, S., Tripp, M. and Varadaraju, N. (2017), "Examining accident reports involving autonomous vehicles in California", *Plos One*, Vol. 12 No. 9, pp. 1-20.

Fiala, E. (1954), "Seitenkräfte am rollenden luftreifen", *VDI-Zeitschrift*, Vol. 96, pp. 973-979.

Giselsson, P. (2010), "Adaptive nonlinear model predictive control with suboptimality and stability guarantees", in *Proceedings of 49th IEEE Conference on Decision and Control*, Atlanta, GA, pp. 3644-3649.

Harris, M. (2016), "Google reports self-driving car mistakes: 272 failures and 13 near misses", available at: www.theguardian.com/technology/2016/jan/12/google-self-driving-cars-mistakes-data-reports (accessed January 12).

Horst, R. and Hogema, J. (1993), "Time-to-collision and collision avoidance systems", in *Proceedings of 6th ICTCT Workshop Safety Evaluation of Traffic Systems: Traffic Conflicts and Other Measures*, Salzburg, pp. 109-121.

Howard, T. (2009), "Adaptive model predictive motion planning for navigation in complex environments", Ph.D. Thesis, Carnegie Melon University.

Jain, V., Kolbe, U., Breuel, G. and Stiller, C. (2019), "Reacting to multi-obstacle emergency scenarios using linear time varying model predictive control", *30th IEEE Intelligent Vehicles Symposium*, Paris, pp. 1822-1829.

Jeong, Y., Kim, K., Kim, B., Yoon, J., Chong, H., Ko, B. and Yi, K. (2015), "Vehicle sensor and actuator fault detection algorithm for automated vehicles", in *Proceedings of 2015 IEEE Intelligent Vehicles Symposium*, Seoul, pp. 927-932.

Ji, J., Khajepour, A., Melek, W. and Huang, Y. (2017), "Path planning and tracking for vehicle collision avoidance based on model predictive control with multiconstraints", *IEEE Transactions on Vehicular Technology*, Vol. 66 No. 2, pp. 952-964.

Li, X., Sun, Z., Zhu, Q. and Liu, D. (2014), "A unified approach to local trajectory planning and control for autonomous driving along a reference path", in *Proceedings of IEEE International Conference on Mechatronics and Automation*, Tianjin, pp. 1716-1721.

Kim, S., Tomizuka, M. and Cheng, K. (2009), "Mode switching and smooth motion generation for adaptive cruise control systems by a virtual lead vehicle", *IFAC Proceedings Volumes*, Vol. 42 No. 15, pp. 490-496.

Kim, S. (1994), "The minimal time detection algorithm", in *Proceedings of 1994 IEEE Aerospace Applications Conference Proceedings*, Vail, CO, pp. 103-115.

Kim, S. (2012), "Design of the adaptive cruise control systems: an optimal control approach", Ph.D. Thesis, UC Berkeley.

Lima, P., Nilsson, M., Trincavelli, M., Mårtensson, J. and Wahlberg, B. (2017), "Spatial model predictive control for smooth and accurate steering of an autonomous truck", *IEEE Transactions on Intelligent Vehicles*, Vol. 2 No. 4, pp. 238-250.

Liu, J., Jayakumar, P., Stein, J. and Ersal, T. (2017), "Combined speed and steering control in high-speed autonomous ground vehicles for obstacle avoidance using model predictive control", *IEEE Transactions on Vehicular Technology*, Vol. 66 No. 10, pp. 8746-8763.

Liu, K., Gong, J., Kurt, A., Chen, H. and Ozguner, U. (2017), "A model predictive-based approach for longitudinal control in autonomous driving with lateral interruptions", in *Proceedings of IEEE Intelligent Vehicles Symposium*, Los Angeles, CA, pp. 359-364.

Mayne, D., Rawlings, J., Rao, C. and Scokaert, P. (2000), "Constrained model predictive control: stability and optimality", *Automatica*, Vol. 36 No. 6, pp. 789-814.

SAE On-Road Automated Vehicle Standards Committee (2016), "Taxonomy and definitions for terms related to driving automation systems for on-Road motor vehicles", Standard J3016.

Svensson, L., Massony, L., Mohan, N., Wardz, E., Brendenx, A., Feng, L. and Törngren, M. (2018), "Safe stop trajectory planning for highly automated vehicles: an optimal control problem formulation", in *Proceedings of IEEE Intelligent Vehicles Symposium*, Changshu, Suzhou, pp. 517-522.

Taoka, G. (1989), "Brake reaction times of unalerted drivers", *ITE Journal*, Vol. 59 No. 3, pp. 19-21.

Thiffault, P. and Bergeron, J. (2003), "Monotony of road environment and driver fatigue: a simulator study", *Accident Analysis & Prevention*, Vol. 35 No. 3, pp. 381-391.

Xue, W., Yang, B., Kaizuka, T. and Nakano, K. (2018), "A fallback approach for an automated vehicle encountering sensor failure in monitoring environment", in *Proceedings of 2018 IEEE Intelligent Vehicles Symposium*, Changshu, Suzhou, pp. 1807-1812.

Yang, K., He, X., Liu, Y., Ji, X. and Chen, D. (2018), "Piecewise Affine-Based shared steering torque control scheme for cooperative path-tracking: a game-theoretic approach", *SAE Technical Paper*, Detriot, MI.

Yoshida, H., Shinohara, S. and Nagai, M. (2008), "Lane change steering manoeuvre using model predictive control theory", *Vehicle System Dynamics*, Vol. 46 No. 1, pp. 669-681.

Zeeb, K., Buchner, A. and Schrauf, M. (2015), "What determines the take-over time? An integrated model approach of driver take-over after automated driving", *Accident Analysis & Prevention*, Vol. 78, pp. 212-221.

Zhao, Z., Chen, W., Wu, X., Chen, P.C.Y. and Liu, J. (2017), "LSTM network: a deep learning approach for short-term traffic forecast", *IET Intelligent Transport Systems*, Vol. 11 No. 2, pp. 68-75.

Corresponding author

Wei Xue can be contacted at: xue-w@iis.u-tokyo.ac.jp